UDC 535.373 + 539.2 + 541.14

E.I. Zenkevich (Minsk, Belarus)
D. Kowerko, C. von Borczyskowski (Chemnitz, Germany)

OPTICAL DETECTION OF SINGLE SEMICONDUCTOR QUANTUM DOTS CdSe/ZnS AND NANOCOMPOSITES BASED ON QUANTUM DOTS AND ORGANIC DYE MOLECULES

In this paper we describe the basic experimental principles of single quantum object detection, mainly of colloidal semiconductor quantum dots CdSe/ZnS and self-assembled nanocomposites based on quantum dots and organic dyes (perylene diimides). We focus also on properties of single quantum dots which can be tuned across the interface to the nanoscopic environment. With respect to quantum dot-dye nanocomposites we discuss structural dynamics and exciton relaxation processes thus providing the data for the development of well-defined multicomponent nanostructures.

Keywords: confocal microscopy, semiconductor quantum dots CdSe/ZnS, perylene bisimides, nanocomposites, blinking, photoluminescence quenching.

Nanostructured materials such a semiconductor quantum dots CdSe/ZnS (QDs) easily exhibit due to their size dependent electronic wave functions (par-

ticle in a box) tuneable optical properties. During the last two decades optical detection of single quantum objects became an exciting break-through experimental approach and is still dramatically developing direction in biology, medicine, nanosensorics and quantum optics. Single quantum object detection offers two more advantages, namely the response to single and/or rare events in the near environment and the application as nanoprobe in heterogeneous materials.

At the beginning we will describe some experimental aspects of single QD detection. The majority of experiments are nowadays performed making use of a reduction of the detection volume which is doped with ultralow ($\leq 10^{-9}$ M) concentrations of QDs. Consequently, QDs are incorporated into thin films or deposited onto surfaces. Photoluminescence (PL) is detected via microscope setups or fluorescence correlation spectroscopy. The detection volume is in this case determined by the confocal volume of the exciting laser which is limited in-plane by the classical optical resolution limit of a few hundred nm and about 1 μm in the perpendicular direction. In the following we will concentrate on "classical" microscopy based techniques [1]. Now we like to make a few remarks with respect to sample preparation. Mostly, QDs are diluted at $C \leq 10^{-9}$ M in appropriate solvents and then spin-coated onto substrates such as quartz

coating leaving QDs spatially well separated > optical resolution) on the substrate. In some cases QDs are diluted in polymers (film thickness is 10÷100 nm).

Typically, a confocal microscope is used in case if several 10÷100 QDs should be investigated simultaneously (Fig. 1). The details are described in [2]. In a confocal detection scheme the laser focus is scanned across the sample while the PL is only detected from the confocal spot.

The emitted light is separated by a neutral beam splitter (3:1). This allows for a spectral and time resolving detection channel in parallel. One part is focused by an achromatic lens to the entrance slit of a monochromator equipped with a CCD at the exit and the other one to a single photon counting avalanche photo diode (APD). The APD signal is splitted to a single photon counting board (time resolution) and to an integration unit. The initial TTL signal (in the fast channel) has to be converted to the fast signal processing standard NIM by a TCSPC (Time Correlated Single Photon Counting) router.

Now we will discuss some characteristic features of single QDs and their application in material science. Typically, upon excitation of many single quantum objects (molecules or QDs) by a constant laser beam PL photons are emitted in bunches separated by a time typical for the residence time in that dark state. This effect is called as PL intermittency (or blinking). Blinking decreases the PL quantum yield and varies for different individual QDs under otherwise the same conditions. The latter indicates a considerable influence of crystal imperfections,

inhomogeneous interfaces (including the impact of ligands or surfactants) and/ or the local (inhomogeneous) environment [3]. An illustrative manifestation of QD PL intermittency is shown in Fig. 2.

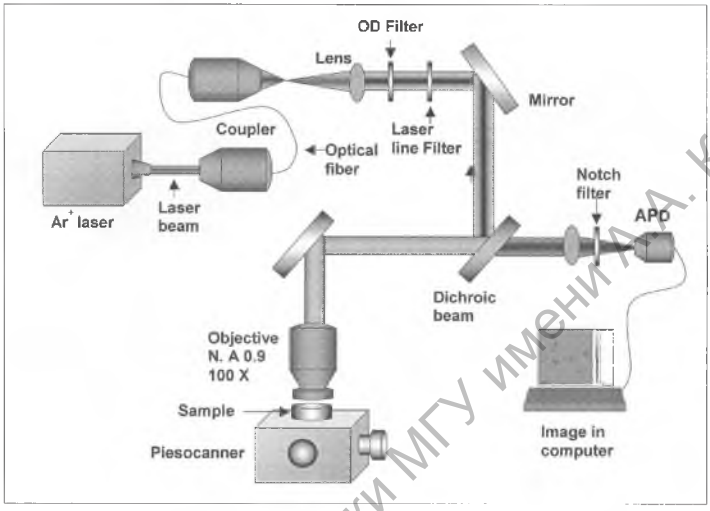

Figure 1. Scheme of a confocal microscope. Main parameters: i) time resolution up to 5 ms/frame, ii) photon rate 5 MHz, iii) excitation intensity 100 W/cm^2, iv) a lateral resolution of 235 nm and a vertical resolution of 970 nm, v) a detection efficiency of 10% for the whole confocal set-up (without the second 50/50-beamsplitter), vi) frames 50000

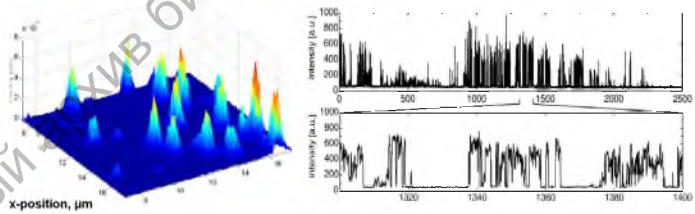

Figure 2. Three-dimensional presentation of PL intensities of single TOPO-capped CdSe/ZnS-QDs on a SiO_2 substrate (A, integration time 1 ms) and appearance of different PL intensities (I_{on} and I_{off}) due to PL blinking (B)

It was found in blinking experiments for single QDs that not only PL intensities are fluctuating but also PL mean decay times since both are inherently related to each other. Fig. 3 shows a direct comparison of PL intensities and (mono-exponentially evaluated) PL decay times during a (threshold based) blinking

time trace with 20 ms binning time. It can be seen that lifetime and intensity are correlated ($I \sim \tau$) that is blinking is not just a digital switching. In addition, a close inspection of the PL reveals that the PL does not decay mono-exponentially across the total intensity range.

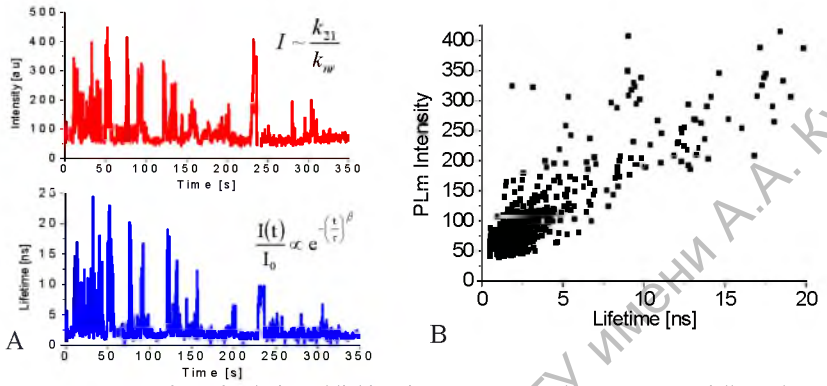

Figure 3. A: PL intensity during a blinking time trace (top) and mono-exponentially evaluated PL decay (life) time of single TOPO-capped CdSe/ZnS QDs in polystyrene at 293 K. Binning time is 20 ms. B: Correlative analysis of PL intensities and decays

Thus, blinking reveals that not only PL intensities are fluctuating but also PL decay times since both are inherently related to each other. If decay times are fluctuating this might indicate that emission stems from different electronic states which are inherently related to different PL energies. Though energy differences might be small and hidden in the linewidth even for a single QD they have been detected as a manifestation of PL spectral diffusion for single QDs [2; 3].

As we have discussed in the previous Section 1.2.3, perylene diimide (PDI) dyes are ideal molecules for single molecule detection. Moreover, we have shown that perylene diimide (PDI) dyes are ideal molecules for single molecule detection (due to a high fluorescence efficiency) and can be appropriately functionalized to form nanocomposites with CdSe/ZnS QDs. Here, for nanocomposites based on Amine-capped QDs and PDI molecules we demonstrate spectral-kinetic observations on the single assembly level which may give additional information concerning the morphology and conformational mobility of PDI molecules attached to the QD surface. Emission spectra related to various statistically formed single nanoobjects are presented in Fig. 4.

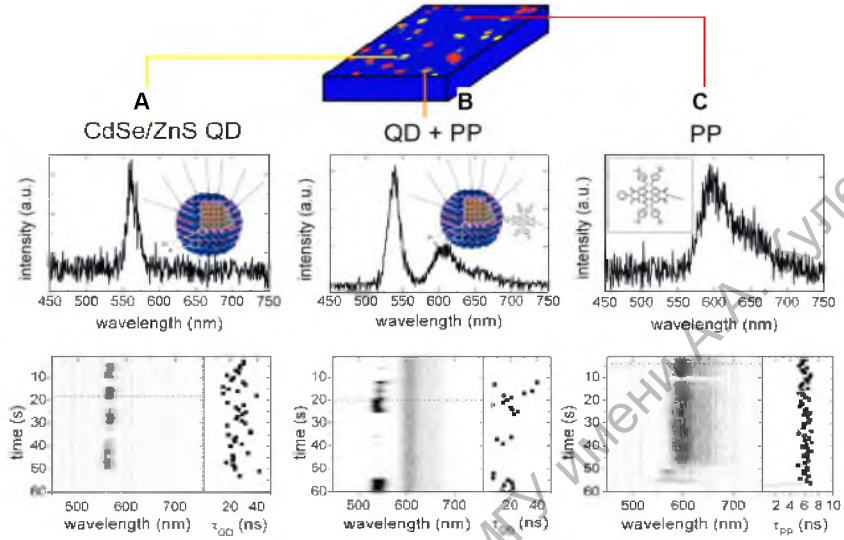

Figure 4. Emission spectra (λ_{exc} = 465 nm; P = 0.6 kW·cm^{-2}) of single amine-capped CdSe/ZnS QD (3 ZnS ML, d_{QD} = 5.1 nm) and (pyridyl)$_1$-PDI molecule (PP). Spectra are related to various confocal spots of the spin-coated sample (1 s binning time) for single QD (**A**), single PP (**C**), and single QD-PDI nanocompo-sites (**B**). PL intensities, spectral positions and decay times τ_{QD} are shown as a function of observation time of 60 s and longer. Single particle sample preparation was done by spin coating a $5 \cdot 10^{-11}$ M solution of the QD-Dye mixture onto a Si/SiO_2 (100 nm thick SiO_2) surface

It was found that the average decay time for single QDs was measured to be $< \tau_D > \approx 20.5$ ns (based on measurements for 20 QDs), while for QDs in a single nanocomposite QD-PP this PL decay was found to be shortened to $< \tau_{DA} > \approx 16$ ns (based on measurements for 18 nanocomposites). The shortening of the decay time is clearly related to the observed decrease of the QD PL intensity upon QD-PP formation. However, the shortening of time cannot be directly related to Foerster resonance energy transfer (FRET) since QD PL decay is intrinsically multi-exponential. Notably, while in a given sample the fluorescence intensity of PP molecule is nearly indistinguishable between PP and attached PP, the QD PL intensity of single QD–PP nanocomposites is quenched on average by 50% as compared to a QD in the same sample (detected at a different position on the surface). Taken together, these facts prove that QD PL quenching is also observed on a single nanoassembly level and reflects directly the existence of an additional non-radiative channel for QD exciton relaxation in these nanoobjects.

Since the PL intensity of the QD is reduced on average by 50 % for each identified single nanocomposite, the corresponding dye induced quenching rate

should be (assuming n = 1) nearly equal to the (average) decay rate of the QD. A close inspection of the time resolved QD PL decay of single nanocomposites provides evidence for the shortening of the QD PL decay time. An average decay time of the multi-exponential QD PL can be estimated using a stretched exponential fit (with $0 < \beta \leq 1$) according to

$$I(t) = I_0 \cdot \exp\left(-\left(\frac{t}{\tau}\right)^{\beta}\right). \quad (1)$$

Thus, an average decay time τ_D for single QDs and single QD-PP nanoassemblies can be calculated according to

$$\tau_D = \frac{\tau}{\beta}\Gamma\left(\frac{1}{\beta}\right). \quad (2)$$

Calculated τ_D values for single QDs and single "QD-PP" nanocomposites as a function of the observation time are shown as black circles in Fig. 4A and 4B. It follows from this analysis that the related quenching efficiency of one dye molecule per QD is obviously broadly distributed between weak and near complete PL quenching.

Additionally, the calculation of the mean value of $\overline{\tau_D}$ by averaging over all nanocomposites leads to the value $\tau_D^A \approx 13.1$ ns for the decay time for QD PL in single QD-PP nanocomposites while it is $\tau_D^D \approx 21.3$ ns for isolated QDs. Correspondingly, an average effective quenching rate k_{DA} can be estimated as

$$k_{DA} = \frac{1}{\tau_{DA}} = \frac{1}{\tau_D^A} - \frac{1}{\tau_{DD}} = 2.9 \cdot 10^{-7}\,s^{-1}. \quad (3)$$

This value is very close to $k_q = 3.5 \cdot 10^{-7}\,s^{-1}$ obtained in bulk experiments for the corresponding QD-PP nanocomposites in titration experiments at $x = 1$ in toluene [1]. Thus, it may be concluded that the reasons of QD PL quenching processes (including low efficiencies of FRET) are very similar in ensemble and single nanoassembly experiments. More concretely, both experimental approaches being applied for QD-Porphyrin and QD-PDI nanocomposites evidently show the existence of strong non-FRET quenching pathways competing effectively with FRET.

Statistical analysis presented in [4] shows that the spectral distribution of PP fluorescence is blue-shifted upon nanocomposites formation. It means that those conformations of PP are favored, for which the bay groups are as much within the molecular plane as possible. Such a situation is reasonable since PP has to be intercalated into the ligand shell which will be more easily accomplished for a nearly flat molecule, since less ligands have to be excluded from the QD surface. Correspondingly, the distribution is shifted from a "free" PP molecule on SiO_2 surface to a "ma-

trix-isolated" type such as in a PMMA film. In addition, spectral fluctuations are enhanced for assembled PP as compared to alone PP molecules in a rigid PMMA film. From this it follows, that the ligand shell imposes more flexibility than in a PMMA film allowing for remaining conformational changes of PP molecules. An alternative explanation is that the curved QD surface allows for more conformational flexibility than on a SiO_2 substrate. The high flexibility of the PP phenoxy side groups on the QD surface is only enabled in absence of steric hindrance.

Concluding, the presented single molecule data reveal that for various QD-Dye nanocomposites, different relative orientations of the PP dyes with respect to the QD surface may be realized, for which the acceptor molecule may have different spectral properties. It means that relative efficiencies of FRET QD→ Dye may differ significantly for each nanocomposite depending on the conformation of the dye attached to the QD surface. Thus, single molecule data provide more specific information on the structure of the QD-PP nanocomposites.

References:

1. Kowerko, D. FRET and ligand related NON-FRET processes in single quantum dot-perylene bisimide assemblies / J. Schuster, N. Amecke, M. Abdel-Mottaleb, R. Dobrawa, F. Würthner, C. von Borczyskowski // PhysChemChemPhys. – 2010. – Vol. 12. – P. 4112–4123.
2. von Borczyskowski, C. Tuning Semiconducting and Metallic Quantum Dots: Spectroscopy and Dynamics / C. von Borczyskowski, E. Zenkevich // Pan Stanford Publishing Pte. Ltd., 2017. – 398 p.
3. Cichos, F. Power-law intermittency of single emitters / F. Cichos, C. von Borczyskowski, M. Orrit // Curr. Opin. Coll. Interf. Science. – 2007. – Vol. 12. – P. 272–284.
4. Zenkevich, E. Self-Assembled Organic-Inorganic Nanostructures: Optics and Dynamics / E. Zenkevich, C. von Borczyskowski // Pan Stanford Publishing Pte. Ltd., 2017. – 408 p.